

# Giant enhancement of photodissociation of polar dimers in electric fields

R. González-Férez<sup>1</sup> and P. Schmelcher<sup>2</sup>

<sup>1</sup>*Instituto Carlos I de Física Teórica y Computacional,  
and Departamento de Física Atómica, Molecular y Nuclear, Universidad de Granada, Spain*

<sup>2</sup>*Zentrum für Optische Quantentechnologien, Universität Hamburg, Germany*

(Dated: June 28, 2018)

We explore the photodissociation of polar dimers in static electric fields in the cold regime using the example of the LiCs molecule. A giant enhancement of the differential cross section is found for laboratory electric field strengths, and analyzed with varying rovibrational bound states, continuum energies as well as field strengths.

## I. INTRODUCTION

The availability of cold to ultracold polar dimers in their absolute ground state [1–3] represents a breakthrough towards the control of all molecular degrees of freedom, i.e., the center of mass, electronic, rotational and vibrational motions. Such a polar sample provides a unique starting point to manipulate the internal structure of molecules, and therefore the molecular dynamics with electrostatic fields. Oriented pendular states present a paradigm in this context. They exhibit a preferred spatial direction of their permanent electric dipole moments, which introduces an anisotropic and long-range electric dipole-dipole interaction between two dimers. Thus, by changing the directional features one can control and manipulate physical processes taking place in the ultracold regime, e.g., scattering dynamics [4–7], chemical reactions [8–11], spin dynamics [12], or even more, create quantum computational devices [13–15].

Here, we investigate a specific process, namely, the dissociation of polar diatomic molecules into two cold atoms via single-photon absorption, and how this process can be controlled and manipulated by using an additional external electric field. As a representative example, we consider the electronic ground state of the LiCs dimer and analyze the direct dissociation within the electronic ground state. The dependence of the angular distribution of the photofragments on the initial rovibrational bound state, on the energy of the continuum, and on the static electric field strength are analyzed in detail. Our focus is the cold regime, where transitions to a few scattering partial waves contribute. In the later case the spectrum shows shape resonances showing up in the fact that, e.g., an initial bound state with rotational quantum number  $J \pm 1$  leads to large field-free differential cross sections and angular distributions via a shape resonance of angular momentum  $J$ . Switching on a static field, the hybridization of the angular motion, i.e., mixing of the rotational states, takes places, and the dissociation process is significantly modified. We demonstrate that a moderate static electric field provokes enhancements of several orders of magnitude of the angular distributions of the dissociation process.

The paper is organized as follows. In Sec. II the rotational Hamiltonian is presented together with the differ-

ential cross section and angular distribution of a direct dissociation process within the electronic ground state. We discuss the numerical results for LiCs in Sec. III, analyzing the field-free and field-dressed cases. The conclusions and outlook are provided in Sec. IV.

## II. THE ROVIBRATIONAL HAMILTONIAN AND THE DISSOCIATION PROCESS

The description of this process is achieved within the Born-Oppenheimer separation of the electronic and nuclear coordinates. We assume that for the considered regime of field strengths a perturbation theoretical treatment holds for the description of the interaction of the field with the electrons, whereas a nonperturbative treatment is indispensable for the corresponding nuclear dynamics. Thus, the rovibrational Hamiltonian of a polar dimer exposed to an homogeneous and static electric field reads

$$H = T_R + \frac{\hbar^2 \mathbf{J}^2(\theta, \phi)}{2\mu R^2} + V(R) - FD(R) \cos \theta \quad (1)$$

where  $R$  and  $\theta, \phi$  are the internuclear distance and the Euler angles, respectively, and we use the molecule fixed frame with the coordinate origin at the center of mass of the nuclei.  $T_R$ ,  $\hbar \mathbf{J}(\theta, \phi)$ ,  $\mu$ , and  $V(R)$  are the vibrational kinetic energy, orbital angular momentum, reduced mass of the nuclei and the field-free adiabatic electronic potential energy curve, respectively. The last term in Eq. (1) provides the interaction between the electric field and the molecule via its permanent electronic dipole moment function  $D(R)$ . The electric field is oriented along the  $z$ -axis of the laboratory frame and posses the strength  $F$ . Our study is restricted to a non-relativistic treatment and addresses the spin singlet electronic ground state.

In field-free space, each bound state of the molecule is characterized by its vibrational, rotational, and magnetic quantum numbers  $(\nu, J, M)$ . In the presence of the electric field only the magnetic quantum number  $M$  is conserved. However, for reasons of addressability we will refer to the electrically dressed states by means of the corresponding field-free quantum numbers  $(\nu, J, M)$ .

We assume a direct dissociation process within the electronic ground state with  $^1\Sigma^+$  symmetry caused by

a beam of linearly polarized light. The polarization of this laser is taken parallel to the direction of the static field. The initial state consists of a rovibrational bound state of the polar dimer exposed to an electrostatic electric field and via the absorption of a photon a transition takes place to a continuum final state. The absorption of the photon from a linear polarized laser is described in terms of perturbation theory. Thus, making use of the dipole approximation the differential cross section is given by

$$\frac{d\sigma}{d\Omega} = \frac{\hbar^2}{2\mu} I(\Omega), \quad (2)$$

with  $I(\Omega) \equiv I(\Omega; \eta, E, F)$  being the angular distribution

$$I(\Omega) = |\langle \Psi_C(\Omega; E) | D(R) \cos \theta | \Psi_\eta \rangle|^2, \quad (3)$$

where  $\Psi_\eta \equiv \Psi_\eta(R, \theta, \phi)$  is the rovibrational bound eigenstate of the Hamiltonian (1). It is characterized by the quantum numbers  $\eta \equiv (v, J, M)$ , i.e.,  $v$  and  $J$  are the field-free quantum numbers of this field-dressed level. The final state  $\Psi_C(\Omega; E) \equiv \Psi_C(\Omega, R, \theta, \phi; E)$  is, in the field-free case, given by [16]

$$\Psi_C(\Omega; E) = \sum_{J'M'} (2J' + 1) e^{i\Delta_{J'M'}} \psi_{J'M'}(R, \theta, \phi; E) \times D_{M'0}^{J'}(\Omega, 0) \quad (4)$$

where  $\psi_{J'M'}(R, \theta, \phi; E)$  is the energy normalized eigenfunction of the Hamiltonian (1) describing the relative motion of the nuclei with kinetic energy  $E = \hbar k^2 / 2\mu > 0$ . It is characterized by the phase  $\delta_{J'M'} = \Delta_{J'M'} + J'\pi/2$  through the relation  $\psi_{J'M'}(R \rightarrow \infty, \theta, \phi; E) \sim \sin(kR + \delta_{J'M'} - \pi J'/2) Y_{J'M'}(\theta, \phi)$ , where  $Y_{J'M'}(\theta, \phi)$  are the spherical harmonics normalized-to-unity. The momentum  $\mathbf{k}$ , with Euler angles  $\Omega = (\Theta, \Phi)$ , represents the propagating vector pointing along the final recoil direction of the photofragments.  $D_{M'0}^{J'}(\Omega, 0) = D_{M'0}^{J'}(\Theta, \Phi, 0)$  is a Wigner rotation matrix [17].

We remark that if we assume the molecular ensemble to be randomly oriented, the population is equally distributed among the states with different values of  $M$ , and using the axial recoil approximation [16], the angular distribution (3) is reduced to the well known expression  $I(\Theta, \Phi) = \sigma(1 + \beta P_2(\Theta)) / 4\pi$ , with  $\beta$  being the anisotropy parameter,  $P_2(\Theta)$  the second-order Legendre polynomial, and it is normalized to the cross section  $\sigma$ . This expression was derived in the pioneering study of R.N. Zare and D. R. Herschbach [18], which was followed by a vast and rich amount of theoretical and experimental works. In particular, several of them have been devoted to the investigation of the photodissociation of oriented molecules [19–26]

Since the probe laser is linearly polarized, we encounter in the absence of the static electric field the selection rules are  $\Delta J = \pm 1$  and  $\Delta M = 0$ . Thus, the angular distribution (3) is reduced to the square of a combination of two Legendre polynomials of degree  $J + 1$  and  $J - 1$ , and it

is symmetric with respect to  $\Theta = \pi/2$ . By turning on the electrostatic field, the hybridization of the rotational motion takes place and only the selection rule  $\Delta M = 0$  holds. We restrict our analysis to initial and final states with  $M = 0$ , and due to the azimuthal symmetry the angular distribution is independent of the Euler angle  $\Phi$ , i.e.,  $I(\Omega) = I(\Theta)$ . In our description, we consider the impact of the electric field on both the continuum and bound levels, and their wave functions are obtained from solving the Schrödinger equation associated to the rovibrational Hamiltonian (1). However, due to the long-range behaviour of the dipole moment,  $D(R) \rightarrow D_7 R^{-7}$ , with  $D_7$  being constant, for  $R \rightarrow \infty$ , the field influence on the continuum states is smaller compared to the bound ones. Thus, we assume that there is no appreciable hybridization of its angular motion, so that the field-free rotational quantum number can be identified, and the expression for the wave function (4) is still holds approximately.

Our aim is to explore the properties of the angular distribution as the initial state, the continuum energy of the photofragments, and the field strength are varied. The two-dimensional Schrödinger equation associated with the nuclear Hamiltonian (1) has been numerically solved by employing a hybrid computational method that combines discrete and basis-set techniques applied to the radial and angular coordinates, respectively [27, 28]. The continuum is discretized and the numerically obtained wave functions are  $L^2$ -normalized. However, the continuum wave functions appearing in Eqs. (3) and (4) are energy-normalized. We address this issue with the help of a time-dependent formalism [27]. The continuum phase is computed by using the fact that our numerical technique selects only those continuum states that are zero on the borders of the discretization box.

### III. RESULTS

We investigate the impact of a static electric field on the dissociation of a polar dimer. As prototype example we take the  ${}^7\text{Li}^{133}\text{Cs}$  dimer in its electronic ground state  $X^1\Sigma^+$ . The potential energy curve is obtained from experiment [29] including the correct long-range behavior. For the electric dipole moment function, we have used semiempirical data [30], which were linearly extrapolated to short distances, and at long distance we have fitted them to the asymptotic behaviour  $D_7/R^7$ . Since  $D(R)$  is negative, in a strong electric field the pendular levels are antioriented along the field direction [27, 31–34]. The electronic ground state of  ${}^7\text{Li}^{133}\text{Cs}$  accommodates 55 vibrational bands, and the last one  $\nu = 54$  has two bound rotational levels with  $J = 0$  and 1 [32]. The continuum spectrum presents a shape resonance with energy  $E \approx 1.36$  mK and rotational quantum number  $J = 2$ . Angular distribution will be provided in atomic units.

Let us first analyze the dissociation process in the absence of the electrostatic field. Figures 1(a) and (b)

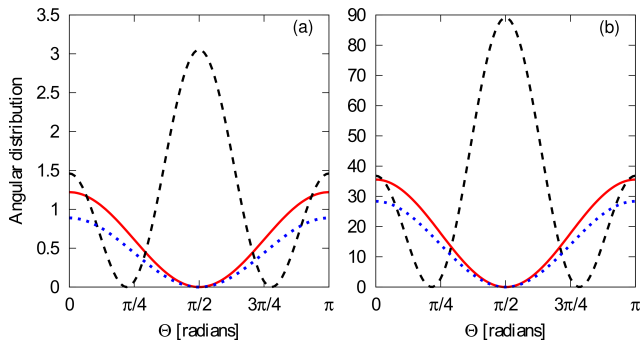


Fig. 1. Field-free angular distribution for the dissociation process to a continuum state with energy  $E \sim 0.3$  mK, the initial states are  $(45, J, 0)$  (a) and  $(50, J, 0)$  (b) with rotational quantum numbers  $J = 0$  (full line), 1 (dashed line) and 2 (dotted line).

present the angular distribution as a function of the angle  $\Theta$  for the initial states with  $\nu = 45$  and 50 and  $J = 0, 1$ , and 2, respectively, and the final continuum energy is 0.3 mK. For a certain rotational quantum number,  $I(\Theta)$  is symmetric with respect to  $\Theta = \pi/2$  and it is a combination of Legendre polynomials. For the  $J = 0$  states, the dissociation is only possible to continuum levels with  $J = 1$ , and  $I(\Theta)$  is proportional to  $\cos^2 \Theta$ . For the  $J = 1$  initial states, the matrix elements of the  $p \rightarrow d$ -wave transitions are larger than the corresponding ones of the  $p \rightarrow s$ -wave transitions. In this case,  $I(\Theta)$  does not have zeros but two minima at small but nonzero values which are shifted with respect to the two nodes of the second order Legendre polynomial. From  $J = 2$  bound states, the final continuum level could have  $J = 1$  and  $J = 3$ , with the transition to  $J = 1$ -levels being dominant, and  $I(\Theta)$  is zero for  $\Theta = \pi/2$ . The quantitatively different values of  $I(\Theta)$  in both panels illustrate its strong dependence on the initial bound state due to the overlap of the bound state wave function with the highly oscillating continuum wave function weighted by the dipole operator. For lower lying rovibrational levels, the differential cross section is therefore significantly reduced.

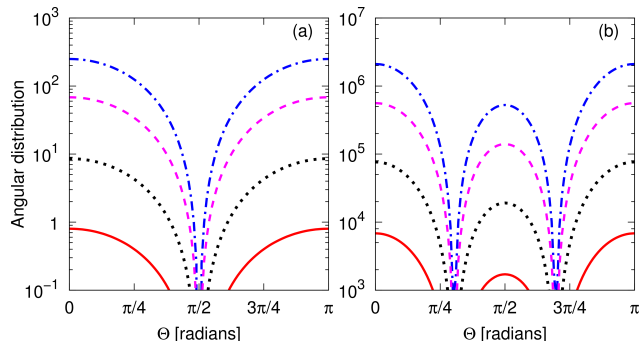


Fig. 2. Field-free angular distribution for the dissociation process to a continuum state with energy  $E \sim 1.36$  mK, which is part of the spectrum where the  $J = 2$  shape resonance appears. The initial states are  $(\nu, 0, 0)$  (a) and  $(\nu, 1, 0)$  (b) with vibrational quantum numbers  $\nu = 40$  (full line), 45 (dotted line), 50 (dash-dotted line), and 52 (dashed line).

The effect of increasing the dissociation energy is manifested in the interplay between the allowed transitions, and, thus, in a variation of  $I(\Theta)$ . In Figs. 2(a) and (b) we present the angular distribution from bound states with  $J = 0$  and 1, respectively, within the vibrational bands  $\nu = 40, 45, 50$  and 52, for a continuum energy in the vicinity of the shape resonance. Note, that a semilogarithmic scale is used to cover the wide range of variation of  $I(\Theta)$ . Taking the bound state belonging to the last vibrational bands gives rise to variations of  $I(\Theta)$  of more than two orders of magnitude. If the continuum energy is increased  $I(\Theta)$  is also increased, as can be seen from a comparison of the results for the bound levels  $(40, 0, 0)$  and  $(50, 0, 0)$  presented in Figs. 1(a) and (b) and those in Fig. 2(a). Due to the field-free selection rules, the transition to the shape resonance is not allowed for the  $(\nu, 0, 0)$  states, whereas it has a dramatic impact on the dissociation from the  $(\nu, 1, 0)$  levels, cf. Fig. 2(b). Indeed,  $I(\Theta)$  shows the same dependence on  $\Theta$  as in Figs. 1(a) and (b), but its absolute value is increased by several orders of magnitude. For the  $(50, 1, 0)$  state, we find  $I(0) = 36.8$  and  $2.1 \times 10^6$  for continuum energies 0.3 and 1.36 mK, respectively. The resonance wave function has a larger probability at short distances, which gives rise to a larger overlap with the bound state wave function. In the absence of the field, this resonance level is also accessible from a bound  $f$ -wave, and the corresponding angular distribution is also significantly increased compared to other spectral regions.

On exposing the molecule to an additional static electric field, the hybridization of the angular motion takes place, the selection rule on  $J$  does not hold any more, and the process of dissociation is altered severely. We focus here on the transition from three bound rovibrational levels within the field-free vibrational band  $\nu = 50$ , and for rotational quantum numbers  $J = 0, 1$ , and 2, with  $M = 0$ , and we consider  $F \leq 10.28$  KV  $\text{cm}^{-1}$ .

Before discussing the results for the angular distributions, it is illuminating to analyze the evolution of the above states as the field is varied. The  $(50, 0, 0)$  level is a high-field-seeker, and for  $F = 10.28$  kV  $\text{cm}^{-1}$ , it shows a moderate orientation with  $\langle \cos \theta \rangle = -0.451$ . In the considered regime of field strengths, the levels  $(50, 1, 0)$  and  $(50, 2, 0)$  are low-field-seekers, and they are not essentially oriented,  $\langle \cos \theta \rangle = 0.021$ , and 0.009, respectively, for  $F = 10.28$  kV  $\text{cm}^{-1}$ . Based on our previous work[32] about highly excited rovibrational levels of LiCs in a static electric field, we can safely assume that the considered field strengths do not yield a significant impact on the vibrational dynamics. Hence, in the framework of the effective rotor approximation [28], for a certain field strength  $F$ , the wave function of the  $(\nu, J, M)$  state can be written as

$$\Psi_{\nu JM}(R, \theta, \phi) \approx \psi_{\nu 0,0}(R) \sum_{j=0}^{N-1} C_{jM}^F Y_{jM}(\theta, \phi), \quad (5)$$

where  $Y_{jM}(\theta, \phi)$  is the normalized-to-unity spherical harmonics with indices  $j$  and  $M$ , and  $\psi_{\nu 0,0}(R)$  are the

field-free vibrational wave function of the state  $(v, 0, 0)$ . The  $C_{jM}^F$  provide the contribution of the partial wave  $(j, M)$  to the rotational dynamics. They depend on the field strength, and satisfy the normalization condition  $\sum_j |C_{jM}^F|^2 = 1$ . Note that the above sum should contain an infinite number of terms, but for reasons of addressability we assume that only the first  $N$  partial waves are needed to properly describe the corresponding dynamics. The evolution of the weights  $|C_{j0}^F|^2$ ,  $j = 0, \dots, 3$  for the states  $(50, J, 0)$  with  $J = 0, 1$  and  $2$  are presented for varying  $F$  in Figs. 3(a), (b), and (c), respectively. For the  $(50, J, 0)$  level,  $|C_{j0}^F|^2$  remains roughly constant and close to 1 for  $F \lesssim 10 \text{ kV cm}^{-1}$ , decreasing thereafter. Moreover, its contribution is dominant for  $F \lesssim 51.4, 25.7$  and  $30.8 \text{ kV cm}^{-1}$  and  $J = 0, 1$  and  $2$ , respectively. The weights of the other partial waves,  $|C_{j0}^F|^2$  with  $j \neq J$ , monotonically increase with increasing  $F$ .

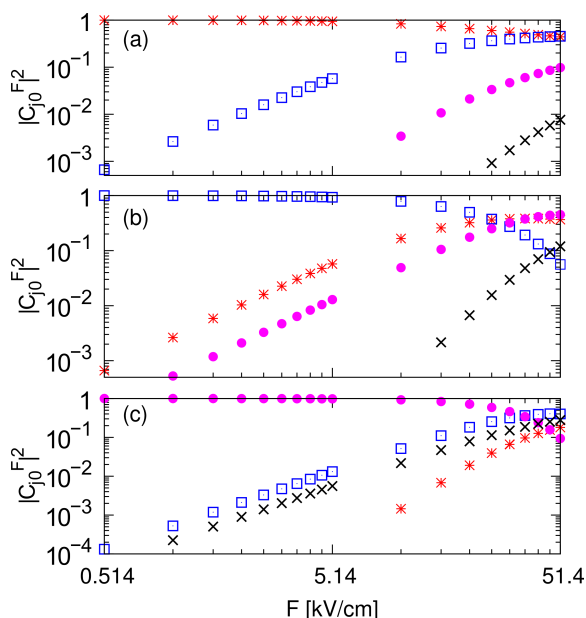


Fig. 3. Contribution of the partial  $s$  (\*),  $p$  ( $\square$ ),  $d$  ( $\bullet$ ), and  $f$  ( $\times$ ) waves to the wavefunctions of the states  $(50, 0, 0)$  (a),  $(50, 1, 0)$  (b), and  $(50, 2, 0)$  (c) as a function of the strength of the static electric field.

Figures 4(a, b), 5(a, b), and 6(a, b) show  $I(\Theta)$  for the two continuum energies  $0.3$  and  $1.36 \text{ mK}$ , and for the initial levels  $(50, J, 0)$  with  $J = 0, 1$ , and  $2$  as well as field strengths  $F = 0, 0.514, 2.57, 5.14$  and  $10.28 \text{ kV cm}^{-1}$ . For the energy  $0.3 \text{ mK}$ , the dissociation process is weakly affected by the field, see Figs. 4(a), 5(a) and 6(a). For the initial bound state  $(50, 0, 0)$ ,  $I(\Theta)$  loses its  $\cos^2 \Theta$ -shape as the field is increased, and it shows significantly larger values for  $\Theta \geq \pi/2$ , compared to  $\Theta < \pi/2$  for  $F \geq 2.57 \text{ kV cm}^{-1}$ , which is due to antiorientation. In particular, we have  $I(0) = 35.6$  and  $42.4$  and  $I(\pi) = 35.6$  and  $49.0$ , for  $F = 0$  and  $F = 10.28 \text{ kV cm}^{-1}$ , respectively. For the  $(50, 1, 0)$  and  $(50, 2, 0)$  states, this effect is only appreciable for  $F = 10.28 \text{ kV cm}^{-1}$ .

If the dissociation takes place to the spectral region

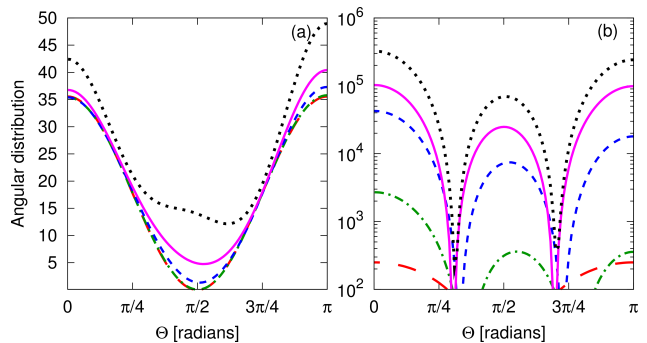


Fig. 4. Field-dressed angular distribution for the dissociation process to a continuum state with energy  $E \sim 0.3 \text{ mK}$  (a) and  $1.36 \text{ mK}$  (b), the initial state being  $(50, 0, 0)$ , and  $F = 0$  (long-dashed line),  $0.514$  (dash-dotted line),  $2.57$  (short-dashed line),  $5.14$  (full line), and  $10.28 \text{ kV cm}^{-1}$  (dotted line).

close to the shape resonance, the additional static field provokes a giant enhancement of the angular distribution of the  $J = 0$  and  $2$  bound states, see Figs. 4(b), and 6(b). For the initial state  $(50, 0, 0)$ ,  $I(\Theta)$  increases by three orders of magnitude when the field is increased from  $F = 0$  to  $10.28 \text{ kV cm}^{-1}$ , and the corresponding value for the angular distribution at zero are  $I(0) = 250$  to  $3.2 \times 10^5$ , respectively. The impact on the dissociation behaviour of the  $(50, 2, 0)$  state is some what reduced: we obtain  $I(0) = 207$  and  $1.6 \times 10^4$  for  $F = 0$  and  $10.28 \text{ kV cm}^{-1}$ , respectively. The large enhancements of the cross sections and angular distributions are due to the field-induced admixtures of  $p$ -wave ( $J = 1$ ) contributions to the  $(50, 0, 0)$  and  $(50, 2, 0)$  states which couple directly to the  $d$ -wave ( $J = 2$ ) shape resonance. Nevertheless, for  $F = 10.28 \text{ kV cm}^{-1}$ , the weight of the  $p$ -wave to the  $(50, 0, 0)$  and  $(50, 2, 0)$  wave functions are still relatively small, with  $|C_{10}^F|^2 = 0.164$  and  $0.051$ , respectively. Note that these large enhancement of the angular distribution are obtained for field strengths which are well within experimental reach. Furthermore, for each vibrational band, exists a field strength that gives rise to the proper hybridization of the angular motion and consequently to an enormous increase of the the dissociation probability for the rotational states  $J \neq 1$  or  $3$ . The angular distribution loses its reflection symmetry with respect to  $\pi/2$  due to the large contribution of the transition to the shape resonance. Analogously to the case of dissociation to the continuum with energy  $E = 0.3 \text{ mK}$ , the angular distribution emerging from the  $(50, 1, 0)$  state is very weakly affected by the external field. The field-dressed  $I(\Theta)$  retains its large values, and only a minor asymmetry is observed for strong fields.

#### IV. CONCLUSIONS

The dissociation of polar molecules in their electronic ground state by the absorption of a single photon to produce two ground state atoms has been investigated

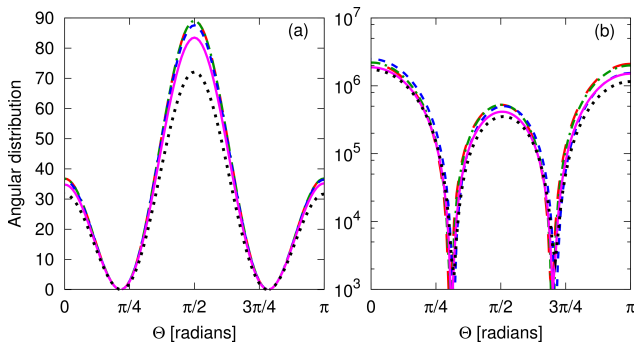


Fig. 5. Same as in Fig. 4 but for the initial state  $(50, 1, 0)$ .

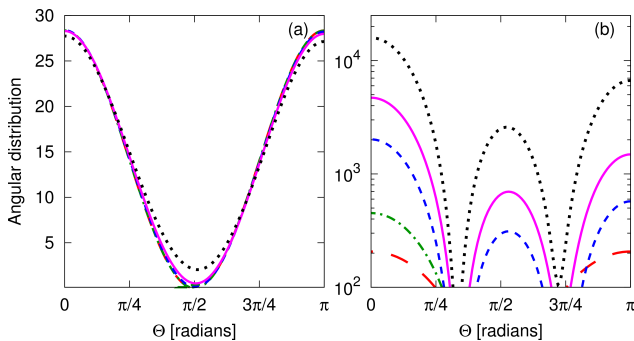


Fig. 6. Same as in Fig. 4 but for the initial state  $(50, 2, 0)$ .

in the presence of an additional electrostatic field, taking as a prototype the LiCs dimer. We have performed a fully rovibrational description of the influence of the electrostatic field on the molecule, whereas the interaction with the laser field has been treated by perturbation theory. We concentrate on the cold regime with continuum energies around 1 mK, and on bound levels being vibrationally highly excited,  $40 \leq \nu \leq 52$ , and rotationally cold,  $J = 0, 1, 2$  and  $M = 0$ . Our study focused in the experimentally accessible range of field strengths  $F = 0.514 - 10.28 \text{ kV cm}^{-1}$ .

In the absence of the electrostatic field, the dissociation

on the cold regime which includes several continuum partial waves such as  $p \rightarrow s$  or  $p \rightarrow d$  transitions. Hence, the angular distribution of the states  $(\nu, J, 0)$ , with  $J = 0, 1$ , and 2 shows values of the same order of magnitude. The field-free  $I(\Theta)$  is a linear combination of at most two Legendre polynomials, being reflection symmetric with  $\Theta$ . A strong dependence on both the bound and continuum states is encountered. The presence of a shape resonance gives rise to an enhancement of several orders of magnitude for the corresponding cross section of those allowed transitions. By turning on an electrostatic field the dissociation process is drastically altered due to the hybridization of the angular motion. The transitions from the states emerging from the field-free  $J = 0$  and 2 states to the shape resonance become allowed and for moderate fields, the corresponding angular distribution is several orders of magnitude larger than its field-free counterpart. Specially, field strengths of a few  $\text{kV cm}^{-1}$  provoke giant enhancements of  $I(\Theta)$  for the initial states  $(\nu, 0, 0)$ , whereas a few tens of  $\text{kV cm}^{-1}$  are needed to observe a similar impact on  $I(\Theta)$  if the process starts from  $(\nu, 2, 0)$  levels.

Although our study focuses on the LiCs dimer and on the direct dissociation taking place within its electronic ground state, we stress that the above-observed physical phenomena are expected to occur equally for other polar molecules. Shape resonances are typical features in the continuum, and their rotational quantum numbers depend on the bound states of the highly excited vibrational bands giving plenty of freedom to the occurrence of the observed enhancement effect.

## ACKNOWLEDGMENTS

We thank Enrique Buendía, Jesús S. Dehesa and Hans-Dieter Meyer, and for discussions. Financial support by the Spanish project FIS2008-02380 (MICINN) as well as the Grants FQM-2445 and FQM-4643 (Junta de Andalucía), Campus de Excelencia Internacional Proyecto GENIL CEB09-0010 is gratefully appreciated. R.G.F. belongs to the Andalusian research group FQM-207.

- 
- [1] K.-K. Ni, S. Ospelkaus, M. H. G. de Miranda, A. Pe'er, B. Neyenhuis, J. J. Zirbel, S. Kotochigova, P. S. Julienne, D. S. Jin, and J. Ye, *Science* **322**, 231 (2008).
  - [2] J. Deiglmayr, A. Grochola, M. Repp, K. Mörtlbauer, C. Glück, J. Lange, O. Dulieu, R. Wester, and M. Weidemüller, *Phys. Rev. Lett.* **101**, 133004 (2008).
  - [3] K. Aikawa, D. Akamatsu, M. Hayashi, K. Oasa, J. Kobayashi, P. Naidon, T. Kishimoto, M. Ueda, and S. Inouye, *Phys. Rev. Lett.* **105**, 203001 (2010).
  - [4] A. V. Gorshkov, P. Rabl, G. Pupillo, A. Micheli, P. Zoller, M. D. Lukin, and H. P. Büchler, *Phys. Rev. Lett.* **101**, 073201 (2008).
  - [5] C. Ticknor, *Phys. Rev. Lett.* **100**, 133202 (2008).
  - [6] T. V. Tscherbul and R. V. Krems, *J. Chem. Phys.* **125**, 194311 (2006).
  - [7] A. V. Avdeenkov, M. Kajita, and J. L. Bohn, *Phys. Rev. A* **73**, 022707 (2006).
  - [8] M. H. G. de Miranda, A. Chotia, B. Neyenhuis, D. Wang, G. Quémener, S. Ospelkaus, J. L. Bohn, J. Ye, and D. S. Jin, *Nature Physics*(2011).
  - [9] G. Quémener and J. L. Bohn, *Phys. Rev. A* **83**, 012705 (2011).
  - [10] G. Quémener and J. L. Bohn, *Phys. Rev. A* **81**, 060701 (2010).
  - [11] R. V. Krems, *Phys. Chem. Chem. Phys.* **10**, 4079 (2008).
  - [12] J. Pérez-Ríos, F. Herrera, and R. V. Krems, *New J. Phys.*

- 12**, 103007 (2010).
- [13] D. DeMille, Phys. Rev. Lett. **88**, 067901 (2002).
- [14] S. F. Yelin, K. Kirby, and R. Côté, Phys. Rev. A **74**, 050301 (2006).
- [15] A. André, D. DeMille, J. M. Doyle, M. D. Lukin, S. E. Maxwell, P. Rabl, R. J. Schoelkopf, and P. Zoller, Nat. Phys. **2**, 636 (2006).
- [16] R. N. Zare, Mol. Photochem. **4**, 1 (1972).
- [17] R. N. Zare, *Angular momentum: understanding spatial aspects in chemistry and physics* (New York: John Wiley and Sons, 1988).
- [18] R. N. Zare and D. R. Herschbach, Proc. I.E.E.E. **51**, 173 (1963).
- [19] R. N. Zare, Chem. Phys. Lett. **156**, 1 (1989).
- [20] S. E. Choi and R. B. Bernstein, J. Chem. Phys. **85**, 150 (1986).
- [21] M. Wu, R. J. Bemish, and R. E. Miller, J. Chem. Phys. **101**, 9447 (1994).
- [22] T. P. Rakitzis, A. J. van den Brom, and M. H. M. Janssen, Chem. Phys. Lett. **372**, 187 (2003), ISSN 0009-2614.
- [23] T. P. Rakitzis, A. J. van den Brom, and M. H. M. Janssen, Science **303**, 1852 (2004).
- [24] A. J. van den Brom, T. P. Rakitzis, and M. H. M. Janssen, J. Chem. Phys. **121**, 11645 (2004).
- [25] A. J. Van Den Brom, P. T. Rakitzis, and M. H. M. Janssen, Phys. Scr. **73**, C83 (2006).
- [26] T. P. Rakitzis and M. H. M. Janssen, Mol. Phys. **108**, 937 (2010).
- [27] R. González-Férez, M. Weidemüller, and P. Schmelcher, Phys. Rev. A **76**, 023402 (2007).
- [28] R. González-Férez and P. Schmelcher, Phys. Rev. A **69**, 023402 (2004).
- [29] P. Staantum, A. Pashov, H. Knöckel, and E. Tiemann, Phys. Rev. A **75**, 042513 (2007).
- [30] M. Aymar and O. Dulieu, J. Chem. Phys. **122**, 204302 (2005).
- [31] R. González-Férez, M. Mayle, and P. Schmelcher, Chem. Phys. **329**, 203 (2006).
- [32] R. González-Férez and P. Schmelcher, New J. Phys. **11**, 055013 (2009).
- [33] M. Mayle, R. González-Férez, and P. Schmelcher, Phys. Rev. A **75**, 013421 (2007).
- [34] R. González-Férez, M. Mayle, and P. Schmelcher, Europhys. Lett. **78**, 53001 (2007).